

Missing-Area Reconstruction in Multispectral Images Under a Compressive Sensing Perspective

Authors: Luca Lorenzi, Farid Melgani, Gregoire Mercier
Publication: IEEE TRANSACTION ON GEOSCIENCE AND REMOTE SENSING, July.2013
Speaker: Hyeong ho, Baek

Short summary: The intent of this paper is to propose new methods for the reconstruction of areas obscured by clouds. They are based on compressive sensing theory, which allows finding sparse signal representations in underdetermined linear equation systems.

I. INTRODUCTION

Clouds in remotely sensed imagery may or may not represent an unwanted source of noise. In case they are viewed as a noise source, several methodologies have been developed in the past in order to cope with this problem. In this paper, they will focus on the approach which attempts to remove the clouds by substituting them with cloud-free estimations.

Recently, CS has been introduced by Donoho and Candes et al. CS theory aims at recovering an unknown sparse signal from a small set of linear projections. By exploiting this new and important result, it is possible to obtain equivalent or better representations by using less information compared with traditional methods.

In this paper, they propose three novel methods to solve the problem of the reconstruction of missing data due to the presence of clouds. Given a cloud-free and a cloud-contaminated image, each of the missing measurements is recovered by applying the CS theory in which cloud-free pixels are exploited.

II. PROBLEM FORMULATION

Let us consider two multispectral images $I^{(1)}$ and $I^{(2)}$ acquired by an optical sensor at two different dates and registered over the same geographical area. Let us suppose that the two acquisitions are temporally close to each other.

We make the hypothesis that image $I^{(2)}$ is obscured by the presence of clouds. We will call cloudy area in image $I^{(2)}$ as target region $\Omega^{(2)}$ and the remaining part as source region $\Phi^{(2)}$. Image $I^{(1)}$ does not contain clouds it is supposed cloud free. Their aim is to generate a new image $I^{(2)}$ without clouds.

They assume that any pixel $x^{(1)} \in \Omega^{(1)}$ can be expressed as linear combination of pixels in region $\Phi^{(1)}$.

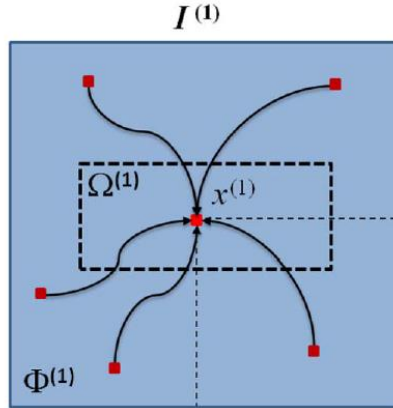


Figure 1 Illustration of the reconstruction principle

In other words, in $I^{(1)}$, we have

$$x^{(1)} = \Phi^{(1)} \alpha \quad \forall x^{(1)} \in \Omega^{(1)} \quad (1)$$

Where α is an unknown weight vector associated with the considered pixel $x^{(1)}$. Once α is computed, if we assume that $I^{(1)}$ and $I^{(2)}$ are temporally close, so that the scene did not change in between the two observations, it will be possible to reuse the α coefficients to reconstruct the spatially corresponding pixel in the missing area $\Omega^{(2)}$.

$$\begin{aligned}
&\text{from } I^{(1)} : \alpha = f\left(\Phi^{(1)}, x^{(1)}\right) \\
&\text{to } I^{(2)} : x^{(2)} = \Phi^{(2)}\alpha
\end{aligned} \tag{2}$$

Where $f(\bullet)$ represents an estimation function.

III. RECONSTRUCTION VIA CS

A. CS solutions

- BP : A well-known solution for problem (1) is the BP principle. It suggests a convexification of the problem by using the L_1 norm. Note that, if the original signal x is sufficiently sparse, the recovery via BP is provably exact.
- OMP : One of the easiest and fastest alternative techniques is the OMP, an improved version of the MP method. MP finds the atom that has the highest correlation with the signal. It subtracts off the correlated part from the signal and then iterates the procedure on the resulting residual signal.
- BP VS OMP : In general, BP and OMP algorithms provide good performances in reconstruction problems. Nonetheless, BP is considered more powerful than OMP, since it can recover with high probability all sparse signals and is more stable. On the contrary, OMP results attractive for its fast convergence and in its ease of implementation.

B. Genetic Algorithm

GA are a part of evolutionary computation which solves optimization problems by mimicking the principles of biological evaluation.

In general, a common GA involves the following steps. First, an initial population of chromosomes is randomly generated. Then, the goodness of each chromosome is evaluated according to a predefined fitness function representing the aim of the optimization. Evaluating the fitness function allows keeping or discarding chromosomes, by using a proper rule based on the principle that, the better the fitness, the higher the chance of being selected. Once the

selection of the best chromosomes is done, the next step is devoted to to the reproduction of a new population. This is done by genetic operators such as crossover and mutation operators. All these steps are iterated until some predefined condition is satisfied. In this situation, the fitness function are given below

$$f_1 = \min \|\alpha\|_0 \quad (3)$$

$$f_2 = \min \|D\alpha - x\|^2 \quad (4)$$

IV. EXPERIMENTAL RESULTS

A. Data set Description and Setup

- Compare the reconstructed image with the original cloud-free image.
- Two aspects : 1. The kind of ground covers obscured and 2. The size of the contaminated area.
- For the purpose of comparison, we implemented two other methods developed to reconstruct cloudy areas in images. One consists in a recent work exploiting a multiresolution inpainting (MRI), whereas the second method estimates a missing pixel by contextual multiple linear prediction (CMLP).

B. Results

- Contamination of Different Ground Covers : In Figure shows mask A covering a region that includes mainly an urban area, mask B obscuring an industrial zone, and mask C covering a vegetation area.

Method	Mask A			Mask B			Mask C		
	PSNR	Complexity	Time [s]	PSNR	Complexity	Time [s]	PSNR	Complexity	Time [s]
MRI	22.54	-	2856	16.05	-	2517	33.77	-	2898
CMLP	20.99	1	1	20.11	1	1	24.05	1	1
OMP	23.96	3	4	20.60	3	4	31.97	3	4
BP	22.22	294	66	24.74	168	59	30.67	301	60
GA	23.78	148	68621	23.15	95	26312	32.01	138	43193

In general, MRI can return visually satisfactory results only when the missing area refers to a uniform region such as a vegetation region.

The OMP algorithm produces very sparse reconstruction solution. On the contrary, the BP algorithm selects a large number of weight coefficients. Finally, GA can be viewed as a compromise between the two previous methods. Despite the very long time needed to estimate the reconstruction model, it results sparser than BP but less parsimonious than OMP.



Figure 2 Masks adopted to simulate the contamination of different ground covers.

- Contamination with different size : Figure shows the three different masks adopted to simulate different increasing cloud cover sizes.

Method	Mask 1			Mask 2			Mask 3		
	PSNR	Complexity	Time [s]	PSNR	Complexity	Time [s]	PSNR	Complexity	Time [s]
MRI	24.27	-	2995	22.85	-	10176	23.82	-	22353
CMLP	24.61	1	1	24.43	1	2	25.46	1	2
OMP	26.36	3	5	26.42	3	16	27.39	3	21
BP	26.45	338	61	26.82	332	143	28.25	329	973
GA	26.72	173	69231	27.10	168	103342	28.15	170	259459

To get higher PSNR values, one needs to resort to CS techniques. Indeed, our implementations return better results in terms of PSNR in all the simulations. The result from this viewpoint underline the main weakness of the GA solution i.e., its expensive computational needs.



Figure 3 Masks adopted to simulate the different sizes of contamination.

V. CONCLUSION

This paper deals with the complex and important problem of removal of clouds from images. First we have shown how two common CS solutions, namely, the OMP and BP algorithms, can be formulated for a cloud-contaminated-image reconstruction problem. Then, we have proposed a solution for solving the CS problem exploiting the capabilities of GA.

The experimental results point out the superiority of the proposed methods compared to two reference methods for cloud removal. OMP has the advantage of being sparser and significantly faster than BP and GA, but it is the less robust method. And BP is much less sparse than OMP. GA represents a good compromise between the OMP and BP methods, mainly because it is more robust than OMP and more sparse than BP.

VI. DISCUSSION

After meeting, please write discussion in the meeting and update your presentation file.

Appendix

Reference

Power and Channel Allocation for Cooperative Relay in Cognitive Radio Networks

Authors: G. Zhao et. al.

Publication: IEEE JSTSP, Feb. 2011

Speaker: Asif Raza

Short summary: In this paper authors mention that cognitive radio relay channels can be divided into three categories: direct, dual-hop, and relay channels. The relay node involves both dual-hop and relay diversity transmission. They develop power and channel allocation approaches for cooperative relay networks. They also develop a low complexity approach that can obtain most of the benefits from power and channel allocation with minor performance loss.

I. INTRODUCTION

Resource (channel and power) allocation in CR relay networks is considered in the paper. The power and channel allocation for cooperative relay in a three-node CR network, which consists of a source, a relay, and a destination and can operate in multiple spectrum bands, is considered. In this context CR relay channels(CRRCs) can be divided into three categories as shown in Fig. 1.

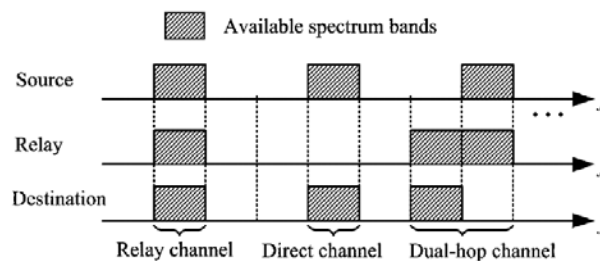


Fig. 1. CRRC in CR networks.

These relay channels have their advantages over each other. For example a dual-hop channel has a bottleneck in throughput whereas a relay channel loses half of its throughput due to its half-duplex constraint. While a CR transmitter and at its intended CR receiver using direct channel on their respective links can result in scarcity of the available spectrum bands for other users in highly congested areas. In this paper authors propose to assign the spectrum band of the relay channel to assist the transmission in dual-hop or direct channels.

Authors in this paper first introduce CRRC in a CR network with four typical spectrum bands, and then discuss power constraints for both the source and the relay. Finally they obtain end-to-end throughput of CRRC.

II. CR SYSTEM DESCRIPTION

A. Cooperative Relay Channel

The network design considered is shown in the following figure.

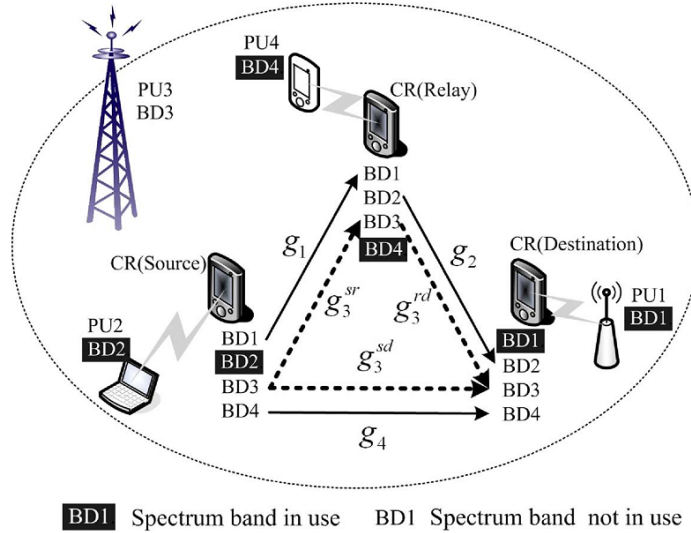


Fig. 2. System setup of cooperative relay in CR networks.

In the network setup every CR node is equipped with an omnidirectional antenna and can simultaneously sense four licensed spectrum bands, BD_i . Each of them belongs to a PU exclusively. The primary user 1 (PU1), PU2 and PU4 are using BD_1 , BD_2 and BD_4 channels respectively. However they have local effect only. The PU3 has large coverage area and effects the whole CR network. However, for example, if PU3 is not transmitting then BD_3 is available to relay node. The source-relay (sr), relay-destination (rd) and source-destination (sd) links are using channel powers over BD_3 as g_3^{sr} , g_3^{rd} and g_3^{sd} respectively.

B. Transmit Power Constraint

Let $\mathbf{P}^S = [p_1^S, p_2^S, p_3^S, p_4^S]$, $\mathbf{P}^R = [p_1^R, p_2^R, p_3^R, p_4^R]$ represents power allocation vectors for source and relay nodes over all four BDs, respectively. The power constraint is defined as:

$p_i^S \leq P_{\max}$, $p_i^R \leq P_{\max}$ and total power is defined as: $\sum_{i=1}^4 p_i^S \leq P_{\max}^S$, $\sum_{i=1}^4 p_i^R \leq P_{\max}^R$ where P_{\max}^S and P_{\max}^R maximum powers that source and relay are able to transmit.

C. End-to-End Throughput

End-to-end throughput on direct transmission on BD4 can be expressed as: $R_{direct} = C(p_4^S g_4)$ where g_4 is channel power over BD4. For dual-hop transmission in BD1 and BD2, both operates serially thus the end-to-end throughput is smaller of two hops, i.e., $R_{dual} = \min\{C(p_1^S g_1), C(p_2^R g_2)\}$. The throughput on relay channel is: $R_{relay} = \frac{1}{2} \min\{C(p_3^S g_3^{sr}), C(p_3^S g_3^{sd}) + C(p_3^R g_3^{rd})\}$. The overall throughput of CRRC is given as: $R_{all}(\mathbf{P}^S, \mathbf{P}^R) = R_{direct} + R_{dual} + R_{relay}$.

III. POWER AND CHANNEL ALLOCATION

Due to complexity, the channel and power allocation is considered independently.

A. *Channel Allocation*: four possible transmission modes are defined as:

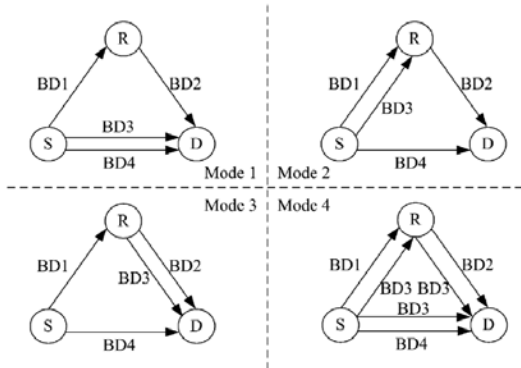


Fig. 3. Different modes of channel allocation.

Objective of channel allocation is to select proper mode to maximize overall end-to-end throughput. The throughput for each mode is defined in end-to-end throughput section. It requires power allocation for each mode.

B. *Power Allocation*: for first 3 modes, power allocation at relay node is defined as:

$$\begin{aligned} J_{RD} &= \max_{\mathbf{P}^R} \left\{ \sum_{i \in \Gamma_{RD}} C(p_i^R g_i) \right\} \\ &= \max_{\mathbf{P}^R} \left\{ \sum_{i \in \Gamma_{RD}} B \log(1 + p_i^R g_i) \right\} \end{aligned}$$

Subject to:

$$\begin{aligned} \sum_{i \in \Gamma_{RD}} p_i^R &\leq P_{\max}^R \\ p_i^R &\leq P_{\max}, \quad i \in \Gamma_{RD} \\ p_i^R &\geq 0, \quad i \in \Gamma_{RD} \end{aligned}$$

Similarly power allocation at source is defined as:

$$J_{SD} = \max_{\mathbf{P}^S} \left\{ \sum_{i \in \Gamma_{SR} \cup \Gamma_{SD}} C(p_i^S g_i) \right\}$$

Subject to:

$$\begin{aligned} \sum_{i \in \Gamma_{SR} \cup \Gamma_{SD}} p_i^S &\leq P_{\max}^S \\ p_i^S &\leq P_{\max}, \quad i \in \Gamma_{SR} \cup \Gamma_{SD} \\ p_i^S &\geq 0, \quad i \in \Gamma_{SR} \cup \Gamma_{SD} \\ \sum_{i \in \Gamma_{SR}} C(p_i^S g_i) &\leq R^* \end{aligned}$$

where $R^* = \sum_{i \in \Gamma_{SR}} C(p_{io}^S g_i)$ represents throughput on link from source to relay node. Similarly the throughput on link from relay to destination can be defined in similar way. Here p_{io}^S represents power allocated to source by using water-filling solution[2], $p_{io}^S = \left[\frac{B}{\ln 2(\lambda + \mu_i)} - \frac{1}{g_i} \right]$. The last constraint in above problem is non-convex.

For mode 1 and 3, the last constraint can be converted into inequality constraint as

$p_1^S \leq \frac{1}{g_1} \left(2^{R^*/B} - 1 \right)$. The problem then becomes convex optimization problem and can be solved by using water-filling solution.

For mode 2 there are more than one spectrum bands for first hop of dual hop transmission. In this case the last constraint of the defined problem is non-convex. It is transformed into equality constraints as:

Step 1: Perform power allocation without considering the constraint and obtain the power allocation vector \mathbf{P}^S .

Step 2: Check whether \mathbf{P}^S meets the constraint. If so, it is the power allocation vector that we need for the source. Otherwise, reduce the sum power constraint of the source P_{\max}^S and perform power allocation until \mathbf{P}^{S^*} meets:

$$R^* - \varepsilon \leq \sum_{i \in \Gamma_{SD}} C(p_i^{S^*} g_i) \leq R^* + \varepsilon \quad \text{where } \mathbf{P}^{S^*} = [p_1^{S^*}, 0, p_3^{S^*}, 0]$$

Step 3: Obtain the inequality constraints by $p_1^S \leq p_1^{S*}$ and $p_3^S \leq p_3^{S*}$

For mode 4: → use SD link (direct transmission) if $g_3^{sd} > g_3^{sr}$ but if $g_3^{sd} \leq g_3^{sr}$ then all three links should be used in relay diversity transmission i.e., $R_{all}(\mathbf{P}^S, \mathbf{P}^R) = R_{direct} + R_{dual} + R_{relay}$

In this case power allocation at relay is: $\mathbf{P}^R(\alpha) = [0, p_2^R(\alpha), p_3^R(\alpha), 0]$ and source needs to divided its power into three parts; direct, dual and relay diversity.

Direct transmission case; $R_{direct}(\alpha) = C(p_4^S g_4)$,

Dual-hop case; $R_{dual}(\alpha) = \min\{C(p_1^S g_1), C(p_2^R(\alpha) g_2)\}$,

Relay transmission; $R_{relay}(\alpha) = \frac{1}{2} \min\{C(p_3^S g_3^{sr}), C(p_3^S g_3^{sd}) + C(p_3^R(\alpha) g_3^{rd})\}$

The overall end-to-end throughput can be maximized as:

$$J(\alpha) = \max_{\mathbf{p}^S} \{R_{direct}(\alpha) + R_{dual}(\alpha) + R_{relay}(\alpha)\}$$

$$\begin{aligned} \text{Subject to: } & \sum_{i \in \{1,3,4\}} p_i^S \leq P_{\max}^S \\ & p_i^S \leq P_{\max}^S, \quad i = 1, 3, 4 \\ & p_i^S \geq 0, \quad i = 1, 3, 4 \\ & p_1^S \leq \frac{g_2}{g_1} p_2^S(\alpha) \end{aligned}$$

- When $C(p_3^S g_3^{sr}) \leq C(p_3^S g_3^{sd}) + C(p_3^R g_3^{dr})$ then objective function becomes:

$$J(\alpha) = \max_{\mathbf{p}^S} \left\{ C(p_1^S g_1) + \frac{1}{2} C(p_3^S g_3^{sr}) + C(p_4^S g_4) \right\}$$

- When $C(p_3^S g_3^{sr}) > C(p_3^S g_3^{sd}) + C(p_3^R g_3^{dr})$ then objective function becomes:

$$J(\alpha) = \max_{\mathbf{p}^S} \left\{ C(p_1^S g_1) + \frac{1}{2} (C(p_3^S g_3^{sd}) + C(p_3^R g_3^{dr})) + C(p_4^S g_4) \right\}$$

In both of the cases, the problem is convex problem and can be solved by using water-filling solution as:

$$p_{1o}^S = \left[\frac{B}{\ln 2(\lambda + \mu_1)} - \frac{1}{g_1} \right]$$

$$p_{3o}^S = \left[\frac{B}{2 \ln 2(\lambda + \mu_1)} - \frac{1}{g_3} \right]$$

$$p_{4o}^S = \left[\frac{B}{\ln 2(\lambda + \mu_4)} - \frac{1}{g_4} \right]$$

In brief, the power and channel allocation in CRRC can be summarized as follows:

- List all possible modes of the channel allocation
- Perform power allocation for each mode
- Pick the mode with the largest overall end-to-end throughput by exhaustive search.

IV. NUMERICAL RESULTS

The parameters used for evaluation are: number of CR nodes=3; number of spectrum bands = 4; spectrum bandwidth = 1 MHz; noise at CR node= -126 dBW; path loss between two CR nodes = 126 dB; maximum allowable power on each spectrum band i.e. $P_{\max}=3W$;

A. Different Source / Relay Power Constraints

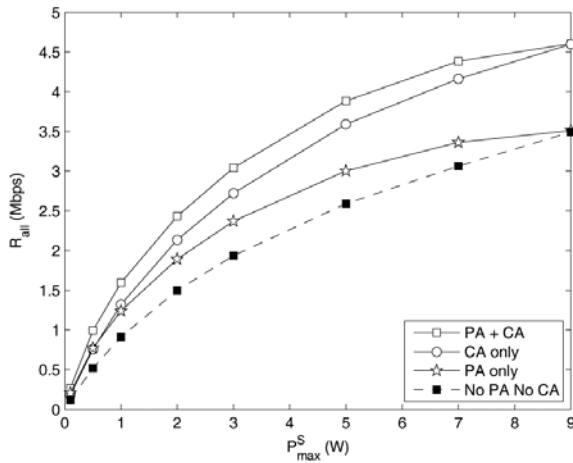


Fig. 4. End-to-end throughput versus the power constraint at the source.

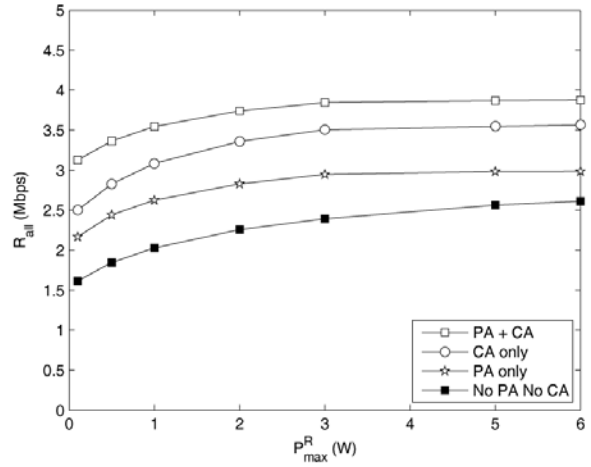


Fig. 5. End-to-end throughput versus the power constraint at the relay.

PA= Power Allocation, CA = Channel Allocation, P_{\max}^S = maximum power at source, P_{\max}^R = maximum power at relay, R_{all} = end-to-end throughput. “No PA No CA” is Mode 4 used as a baseline for comparison. The notable observation in Fig. 4 is that CA continue to increase throughput for increase in sum power constraint however PA can only improve throughput when $P_{\max}^S \leq 9W$. This is because when the sum power constraint is large enough, the per band power constraint will limit the transmit power. {Then the source sends signals with maximum allowable transmit power on each spectrum band. This is equivalent to equal power allocation, i.e., P_{\max} no power allocation.} Therefore, channel allocation is more effective than power allocation in CRRC. In Fig. 5 the throughputs of different schemes grow almost at similar scales. However when the sum power constraint is large enough, the throughput will be capped by per band power constraint.

- A. Low Complexity Approach: if the CR system works in Mode 4, the relay has to conduct both *dual-hop* and relay diversity transmission, which *complicates the system*. Therefore, we omit Mode 4 and only consider Modes 1, 2, and 3 for the power and channel allocation.

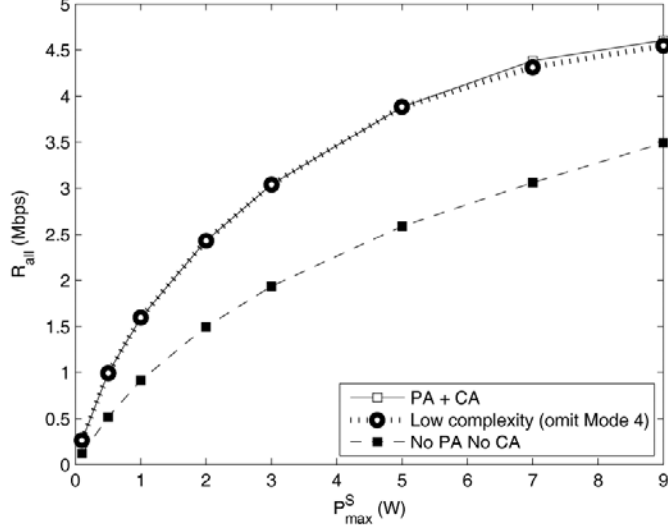


Fig. 6. Performance of the low complexity approach in the typical case with four spectrum bands.

We can find that the low complexity approach of omitting Mode 4 has similar performance to the method of considering all four modes. Furthermore, when the sum power constraint at the source is larger than 9 W, it only decreases the throughput from about 4.6 Mbps to about 4.5 Mbps compared to the scheme with power and channel allocation, i.e., about 2% performance loss.

B. Performance in Multiple Spectrum Bands:

When N independent spectrum bands are used, there are $L=N/4$ relay channels on average. It is shown in fig. 7 that low complexity scheme has performance close to power and channel

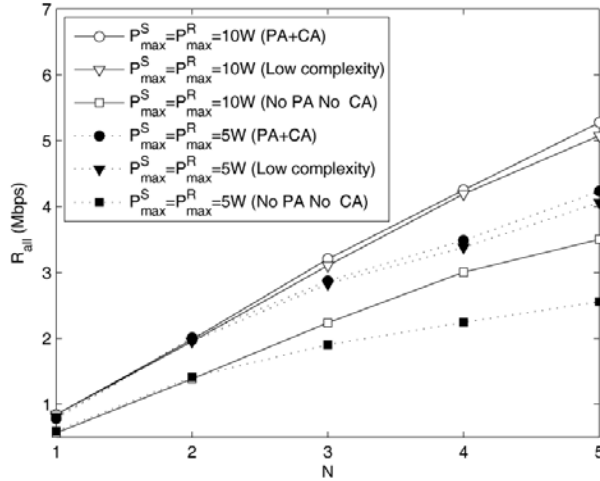


Fig. 7. Performance of the low complexity approach in the case with N spectrum bands.

allocation scheme for both 5W and 10W sum power constraints. Moreover it outperforms the scheme with no power and channel allocation in both of the power constraint cases.